

Wireless Monitoring of Workpiece Material Transitions and Debris Accumulation in Micro-Electro-Discharge Machining

Mark T. Richardson, *Member, IEEE*, and Yogesh B. Gianchandani, *Senior Member, IEEE*

Abstract—Wireless signals are inherently generated with each discharge in micro-electro-discharge machining (μ EDM), allowing direct observation of discharge quality. While traditional methods of monitoring machining quality rely on electrical characteristics at the discharge supply terminals, the wireless method provides more accurate information because it is less affected by electrical parasitics in the supply loop and by spatial averaging. The depth location of a metal–metal interface can be distinguished in the wireless signal. This is useful for determining the stop depth in certain processes. For example, in machining through samples of stainless steel into an electroplated copper backing layer, the metal transition is identified by a 10-dBm change in wireless-signal strength for the 300–350-MHz band and a 5-dBm average change across the full 1-GHz bandwidth. As debris accumulate in the discharge gaps, shifts in the wireless spectra can also indicate spurious discharges that could damage the workpiece and tool. For example, when copper micromachining becomes debris dominated, the 800–850-MHz band drops 4 dBm in signal strength, with a 2.2-dBm average drop across the full 1-GHz bandwidth. [2009-0109]

Index Terms—Batch-mode micromachining, process monitoring, spurious discharges, stainless-steel machining, wireless feedback control.

I. MOTIVATION AND BACKGROUND

MICRO-ELECTRO-DISCHARGE machining (μ EDM) is a technique that utilizes sequential spark discharges to micromachine any conductive material [1]. A cathodically biased machining tool and an anodically biased workpiece are immersed in a dielectric while controlled discharges are fired between these elements. The workpiece thermally erodes much faster than an appropriate tool. In serial-mode μ EDM, the tip of a sharpened wire is used as the machining tool, whereas in batch-mode μ EDM, this function is served by lithographically patterned metal features on a microchip [2]. While μ EDM is

routinely used for a variety of workpiece materials, it can be particularly helpful for materials that are difficult to physically machine, such as tungsten carbide. Within the domain of MEMS devices, μ EDM has permitted the use of stainless steel as a structural material. This is useful not only for its mechanical and thermal properties but also for its biomedical compatibility. Minimum feature sizes of 5 μ m and tolerances of 0.1 μ m are possible. Applications for μ EDM include gas injection nozzles, inkjet printer heads, dc-to-dc boost converters [3], and implantable medical devices such as cortical electrical probes [4] and the antenna stent [5]. Despite the high promise of μ EDM technology, there is room for improvement if it is to be used for high-precision micromachining in a reliable and repeatable way. In this paper, we explore how wireless monitoring of the μ EDM process can help to address two significant challenges: interface sensing and debris accumulation sensing.

A. Metal–Metal Interface Sensing

During the machining process, there are many cases in which the device layer is backed by another conductive layer. A thin device layer may need to be bonded to a handle wafer to prevent deformation. Alternatively, the device layer may have a support layer that is electroplated or physically secured to it. A support layer prevents excessive widening of a machined gap on the distal side of the workpiece and also prevents machining into the stage below the workpiece. For example, a 25- μ m-thick stainless-steel device layer may be backed by 30 μ m of electroplated copper for rigid support during the machining step and subsequent handling. Without it, past work from our group has shown that the dimensional accuracy and precision may be compromised [6].

In batch-mode μ EDM, a metal–metal interface is typically obscured from visual inspection by the tool. For precision machining, real-time information about when the cutting tool reaches the interface of metals would prevent unnecessary damage to the tool and workpiece, as well as reduce machining and characterization time (Fig. 1). In the presence of composite layers, it would be useful to have the equivalent of an electrochemical etch-stop signal for μ EDM for detecting the material transition as the tool advances into the workpiece [7]. Automated detection would reduce the need for detailed characterization when machining a new pattern, changing individual machining steps within a multistep process, or accounting for wear rate after multiple uses of the same tool.

Manuscript received April 28, 2009. First published December 8, 2009; current version published February 3, 2010. This work was supported in part by the National Science Foundation (NSF), in part by the NSF Engineering Research Center for Wireless Integrated Microsystems, and in part by the University of Michigan, Ann Arbor. The work of Y. Gianchandani was supported by the Independent Research/Development Program while he was with NSF. Subject Editor N. de Rooij.

The authors are with the Department of Electrical Engineering and Computer Science, University of Michigan, Ann Arbor 48109 USA (e-mail: mtrichar@umich.edu; yogesh@umich.edu).

Color versions of one or more of the figures in this paper are available online at <http://ieeexplore.ieee.org>.

Digital Object Identifier 10.1109/JMEMS.2009.2035642

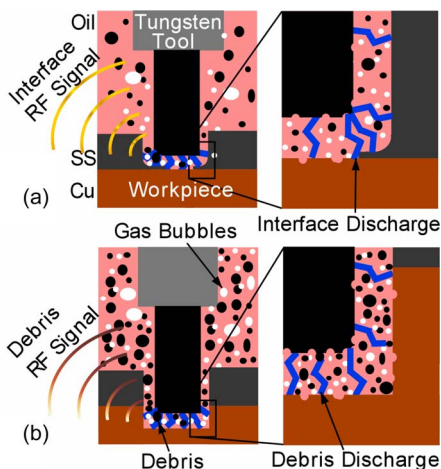


Fig. 1. (a) Tungsten tool of 300 μm diameter produces different wireless signals at the interface of stainless steel and copper. (b) Signal from debris discharges also differs. (Blue) Electrodischarges. (Black) debris. (White) bubbles.

B. Sensing Debris-Dominated Machining

Another major challenge with μEDM is that debris accumulation can severely degrade machining performance for high-density patterns, enclosed patterns, or deep machining [8]–[10]. Debris are created naturally during the discharge process, but problems occur when it is not flushed out of the discharge gap efficiently. The presence of debris can lead to spurious discharges, causing the discharge gap to increase, tool dimensions to decrease, and machining precision to be reduced [11], [12]. In batch-mode μEDM , this is very problematic because the path for debris to escape can be quite tortuous and becomes worse as feature density is scaled up [2].

Various methods of debris flushing have been attempted in the past. In serial mode, rotation and direct oil flushing are the traditional techniques and are effective for most features. Vertical stage vibration is an attractive option for batch-mode flushing. Orbital stage movement (which involves both vertical and lateral motions) has also been used, but this increases the minimum spacing between features. While these methods reduce the accumulation of debris, monitoring the accumulation continues to present a challenge.

The conventional methods for monitoring EDM typically use analysis of voltage and current waveforms on the workpiece (anode) and tool (cathode) sides [13], [14]. In the context of μEDM , this can compromise the machining quality because the addition of a voltage/current probe to the terminals could add a parasitic load that not only influences the accuracy of the measurements but also increases the discharge energy. A larger discharge energy increases the workpiece surface roughness and the discharge gap. Measuring high-frequency waveforms through such probes can be a challenge. Additionally, because the discharge process is stochastic, the shape of these waveforms can vary widely from discharge to discharge, making it difficult to reliably derive information from them. As will be shown later, the variability increases when effects like debris accumulation occur. These methods generally categorize the waveforms into spark discharge, arc discharge, open circuit, or short circuit. Some also track the discharge frequency. Recently, fuzzy analysis and neural network process control methods

have been applied to macroscale EDM [13], [15], [16]. These methods require their own sample size and window calibration in order to filter out noise from the desired trends. One application of this type of monitoring is in dynamic parameter adjustment during machining to ensure that the workpiece entrance and exit holes have consistent sizes [17].

Wireless measurement of the discharge behavior does not affect terminal parasitics and directly measures the discharge. Wireless signals generated from fast current spikes have been studied in the past [18]–[20]. Marconi utilized spark discharges that were similar to those found in EDM for wireless communication in the 1890s. It has also been shown that the noise waveform of discharges between switch contacts is influenced by the choice of material [21] and electrode area [22]. In the late 1970s, early work showed that it was possible to use RF transmissions to distinguish between open-circuit, spark, arc, and short-circuit conditions in macroscale serial-mode EDM [23], [24]. At the microscale, particularly for batch mode, process monitoring is even more critical. Due to the smaller dimensions, tighter tolerances, and electrode multiplicity, the role of debris accumulation and gas evolution can have a much larger impact on discharge quality, which may appear in the wireless spectra [25]. The role of tool wear on depth accuracy is also much more pronounced.

In this paper, we explore the use of wireless signals inherently generated by μEDM discharges to monitor the machining process.¹ Specifically, we investigate the detection of an interface of two metals [Fig. 1(a)] and the discharge quality when debris accumulation occurs during deep machining or in enclosed patterns [Fig. 1(b)]. A view toward monitoring large-scale production by μEDM is considered. Stainless steel is used as the device layer to demonstrate application to high-volume medical device materials.

Section II describes the experimental results for wireless sensing of metal–metal interfaces. Section III describes the sensing of debris accumulation. Section IV is a discussion of the results, and Section V provides the conclusions.

II. METAL–METAL INTERFACE SENSING

Stainless steel of around 100 μm thickness is commonly used in the manufacture of cardiovascular stents. This provides a suitable application context for the proposed technology. The change in wireless RF discharge spectra at the interface between a #304 stainless-steel workpiece and a copper support layer was investigated. After electroplating approximately 60 μm of copper on the backside of 100- μm stainless-steel foil, the steel side was repeatedly machined with a 300- μm -diameter circular tungsten tool at different discharge energies. The machining instrument was a Panasonic ED-72W μEDM . The machining parameters for the experiments are listed in Table I. The presented data are for 80 V and 100 pF, but the other configurations gave similar results. Debris were not allowed to accumulate significantly in this paper. A vertical dither motion of approximately 10- μm amplitude was used for flushing. In contrast with some of the other types of motion,

¹Portions of this paper have appeared in conference abstract form [26].

TABLE I
MACHINING CONDITIONS

Tool Diameter	300 μm
Voltage	70, 80, 110 V
Capacitor	100 pF, 3.3 nF
Resistor	1 k Ω
Z-Feed	0.2, 0.3 $\mu\text{m/s}$

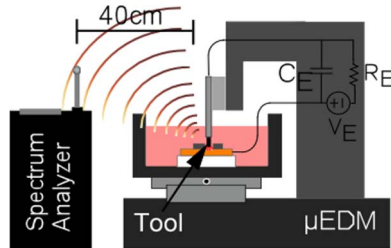


Fig. 2. Experimental setup for wireless monitoring. A spectrum analyzer with dipole antenna receives wireless signal at a distance of 40 cm from the discharge site. Discharge energy is controlled with C_E , R_E , and V_E .

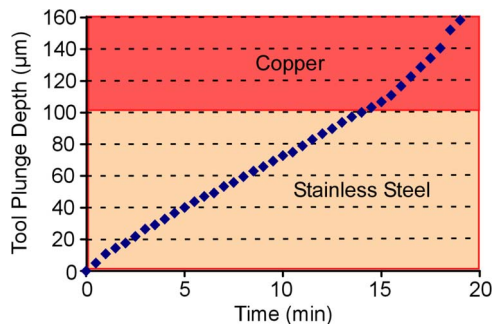


Fig. 3. Traditional way for monitoring machining progress. Tool plunge depth versus time does not unambiguously indicate the location of the interface between steel and copper.

this is compatible with both serial- and batch-mode μEDM . Using a serial-mode tool with batch-mode flushing eliminated the need for a UV LIGA process run to generate a batch-mode tool.

The experimental setup is shown in Fig. 2. An Agilent ESA4405B spectrum analyzer with a dipole antenna was used to periodically monitor the wireless spectrum of discharges at a distance of 40 cm from the machining area. Measurements spanned a bandwidth from 9 kHz to 1 GHz with 10-kHz resolution and 5-dB attenuation. Because there are thousands of discharges per second, the spectra have some random variation. The “max-hold” setting was used over each 30-s interval, selecting the maximum value from approximately 232 samples per data point. This approach captures changes in the maximum discharge energy that could be lost by using a sample averaging approach. Tool plunge depth information was recorded from the μEDM controller, and at the same time, spectral data points were recorded.

As can be seen in Fig. 3, the plot of tool plunge depth versus time does not readily indicate the interface depth, which is often difficult to judge blindly for deep machining. This is because tool plunge depth is affected by tool wear and does not always represent the true machined depth. Because the machining is relatively shallow and the pattern is simple in this experiment, there should be little tool wear, except for edge rounding. The

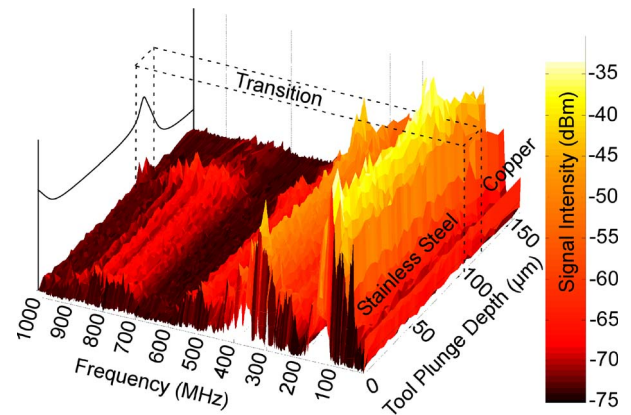


Fig. 4. Three-dimensional plot of received wireless RF signal intensity from machining 100- μm -thick stainless steel with electroplated copper on the backside shows a disturbance across the entire bandwidth at the interface depth.

spectrogram for the stainless-steel/copper interface in Fig. 4 shows a 10-dBm change at around 100 μm in the 300–350-MHz band and a 5-dBm average change across the entire 1-GHz bandwidth. The transition region indicates when the interface is completely past. Tool rounding at the edges requires machining that is deeper than the interface to remove burrs at the bottom of the workpiece (Fig. 1). This effect is a simple amplitude shift that occurs across almost the entire bandwidth. The tool plunge rate plot indicates that the machining was smooth through the entire thickness of the experiment. If there were debris effects, there would have been a noticeable decrease in plunge rate. The shift in amplitude across the band must have been therefore caused by the interface of materials.

The SEM images in Fig. 5 demonstrate the impact of the copper support layer on batch μEDM machining performance. Fig. 5(a) shows a 25- μm -thick stainless-steel antenna stent pattern machined with an $\sim 30\text{-}\mu\text{m}$ electroplated copper support layer on the backside of the workpiece and a passivated sidewall coating on the tool [11]. A close-up in Fig. 5(b) with the support layer and coating shows well-defined edges and a full release. The steel is released from the copper using nitric acid. Fig. 5(c) shows the same pattern, machined without the support layer and tool coating (adapted from [6]). The result has rounded edges and only a partial release.

In order to further investigate the stainless-steel/copper interface, SEM images were taken shortly after the transition from steel to copper in one of the runs. As can be seen in Fig. 5(d), the steel is machined through the entire thickness, and the copper has signs of discharges. There is a slight separation between the copper and steel around the edges. The SEM image in Fig. 5(e) shows an opening in the steel device layer just after the machining has penetrated the steel to the copper backing layer. This technique enables blind monitoring of the actual machined depth, reducing the time required for process characterization of complex patterns.

III. SENSING DEBRIS-DOMINATED MACHINING

To investigate whether performance degradation from debris could be monitored wirelessly, a series of experiments was conducted by machining deep into 1-mm-thick copper at various

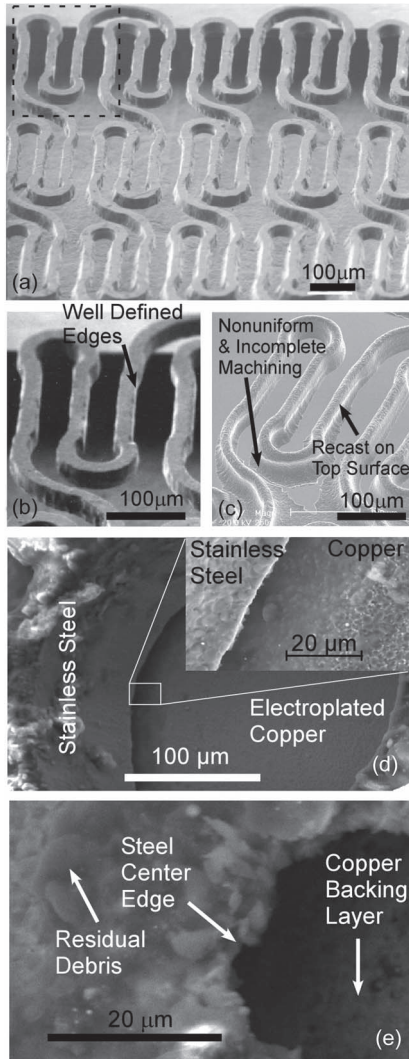


Fig. 5. Impact of electroplated copper support layer during batch μ EDM. In (a), a 25- μ m stainless-steel foil antenna stent pattern is supported with \sim 30- μ m copper during machining. (b) Support layer enables well-defined edges and a full release. (c) When machining without a support layer, only a partial release is achieved with uneven machining (adapted from [6]). (d) Test pattern from the wireless monitoring experiments at the steel/copper interface. Machining was stopped before the full thickness of the copper was traversed. (e) Steel is opening at the center of the machining area just after penetration to the copper backing layer. The exposed steel edge concentrates the electric field and attracts discharges, widening until it reaches the full diameter.

discharge energies while recording the wireless spectra. The goal of the experiments was to determine how the wireless spectrum differs due to debris accumulation over varying discharge conditions and a wide bandwidth.

Debris were allowed to accumulate on the surface of the workpiece without flushing it away. Thick (1-mm) pieces of copper were clamped to form a barrier around the tool and machining site, limiting the volume of oil that was available to flush the discharge gap. Eventually, the volume was saturated with debris. This simulates situations where debris are trapped within the discharge gap due to dense or enclosed patterns or deep machining. The Panasonic MG-ED72W μ EDM controller detects debris accumulation as a short circuit between the tool and workpiece and retracts the tool well past the point that the condition is removed. It then progresses again until another

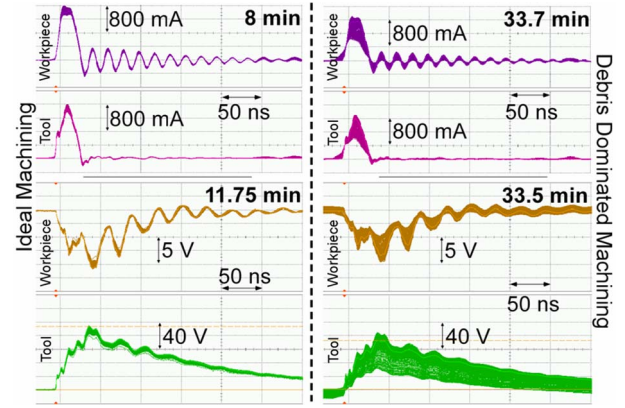


Fig. 6. (Upper) Current and (lower) voltage traces for a tool cathode and workpiece anode during (left) ideal machining and (right) debris-dominated machining. Instability in the debris-dominated machining waveforms indicates that spurious discharges are occurring.

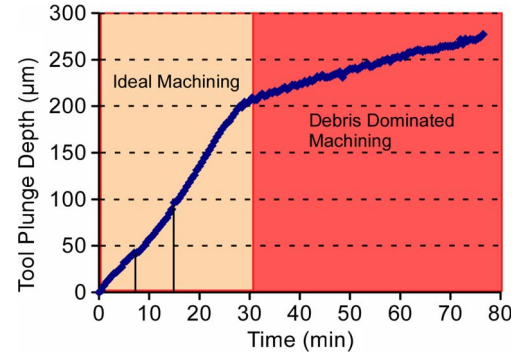


Fig. 7. Tool plunge depth versus time shows debris effects on machining at 30 min.

short circuit is encountered, repeating the process. This routine allows machining to progress but at a lower plunge rate; it does not eliminate the underlying cause of debris accumulation.

For this portion of the effort, the machining tools were also 300- μ m-diameter circular tungsten, and the stage was dithered vertically by approximately 10 μ m. For comparison purposes, voltage and current terminal probes were monitored concurrently (Fig. 6), along with tool plunge depth (Figs. 7 and 9). The data presented here contrast typical runs with low-energy (80-V, 100-pF) discharges used for precision features and high-energy (110-V, 3.3-nF) discharges for a faster rougher finish.

For low-energy discharges, there was a significant decrease in plunge rate at around 30 min, which indicates debris-dominated machining (Fig. 7). The current and voltage traces in Fig. 6 show discharges before and after this decrease. Each trace is the average of 16 samples, but in this plot, multiple traces are shown by using the persistence mode for approximately 30-s intervals. The traces for debris-dominated machining show significant instability compared to ideal machining, even with averaging. The spectrogram in Fig. 8 confirms that there is a significant disturbance in the wireless spectra at the same time. For example, the 800–850-MHz band dropped 4 dBm in signal strength when machining became debris dominated. There was a 2.2-dBm average drop across the full 1-GHz bandwidth. There were also several smaller changes in plunge rate that appeared in the spectra.

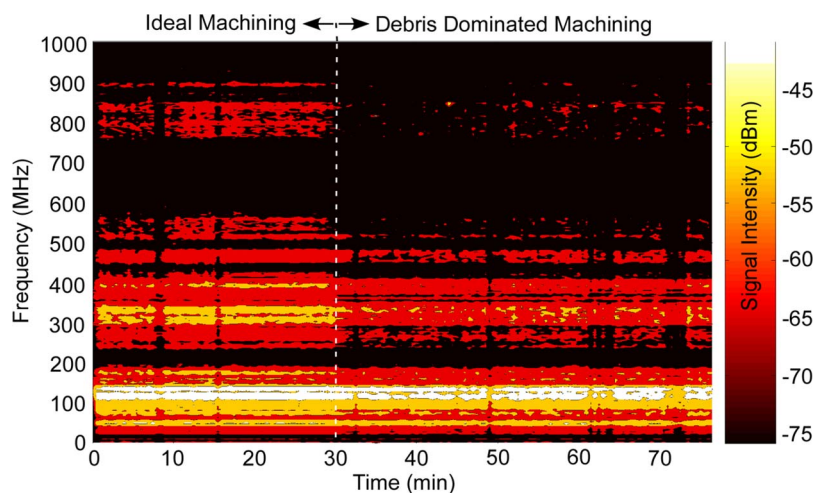


Fig. 8. Received RF with a Cu sample and 300- μm W tool machining with 80 V and 100 pF. At 30 min, a significant signal drop (7.4 dBm max) is detected, indicating debris-dominated machining.

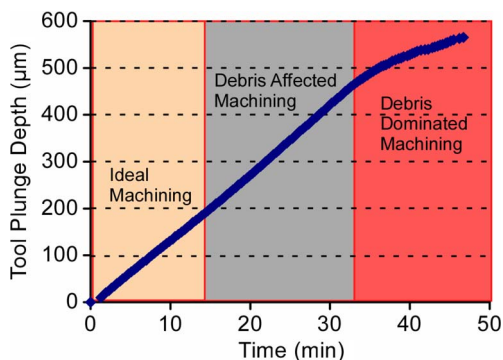


Fig. 9. Tool plunge depth versus time shows debris effects on machining only at 33 min. This is later than 14 min in Fig. 10.

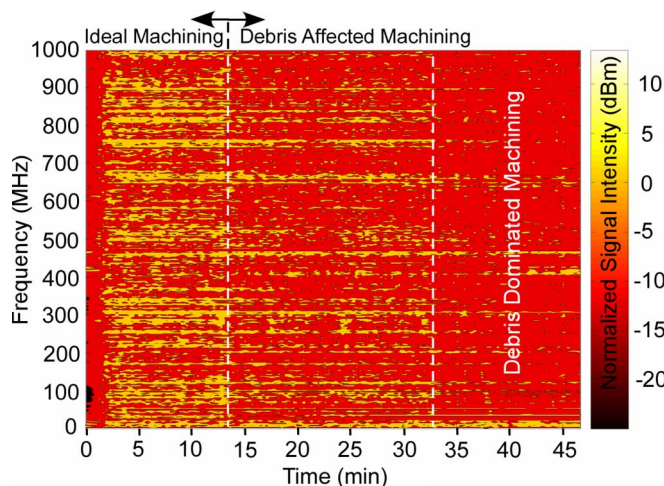


Fig. 10. Received RF signal of high-energy discharges normalized to initial intensity. At 14 and 33 min, there are significant signal drops, indicating debris-dominated machining.

The spectrogram data in Fig. 10 for high-energy discharges were normalized to the first few spectra to show an alternative form of the data. There was a sharp drop in signal intensity around 14 min across almost the whole bandwidth. This was not visible in the tool plunge rate plot of Fig. 9. At around 33 min, the plunge rate decreased, which was also recorded in the

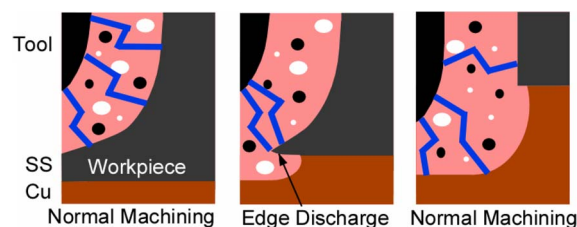


Fig. 11. Hypothesized machining progress at the interface of two metals. Normal machining leads to wear that rounds out the tool. Then, the first layer is punched through in the middle, and discharges concentrate at the edges. Finally, the edge levels out, and normal machining resumes.

spectra. This indicates that, for higher energy discharges, there can be changes that are visible in the wireless spectra before short circuits are detected, which decrease the plunge rate.

IV. DISCUSSION

A. Metal–Metal Interface Sensing

By the time the tool machines through the device layer in the metal–metal interface experiments, the edges are rounded by normal tool wear [27]. The rounded shape is transferred to the workpiece and thus “punches through” at the center of the metal before the outer edges, as shown in Fig. 11. The discontinuity between the metals may form an edge that provides the transitional discharge path with the measured wireless characteristics [28]. Discharges preferentially occur at the edges of the opening and with higher current until the opening has reached the full diameter of the tool plus the discharge gap. Because the wireless measurements use the “max-hold” function over a 232-sample window, these discharges are captured and dominate the spectrum. If an averaged signal were to be used, these spectra would not stand out very readily because normal discharges also occur.

This effect can be corroborated by observing the machining of a slot in serial-mode μEDM . During slot machining, the workpiece stage is dithered along one axis while the tool remains stationary, allowing observation of the machined area with each pass. A tool that is worn at the edges penetrates through the center of the workpiece first, and the discharges

visibly concentrate at the newly formed edges. The opening then becomes progressively larger until it is the same diameter as the tool plus the discharge gap. The higher energy edge discharges are audibly louder than normal discharges at high (110 V) voltages. A similar effect recorded in terminal-probe traces was also independently reported in [29]. As the hole expands, there are many more edge discharges, and the wireless-signal amplitude increases. Eventually, the edge reaches its maximum perimeter and starts to decrease, and the wireless signal follows, lowering in amplitude. This period of edge machining corresponds to the transition region in the wireless spectrogram.

The advantage of this approach for interface detection is that an amplitude disturbance across the entire wireless spectra is a simple signal to detect, even with significant variation from discharge to discharge. While this signal should also be visible in terminal-probe measurements, wireless detection has inherent benefits. Wireless detection has the potential to enable monitoring of multiple machines in parallel while being decoupled from the discharge process.

The edge-discharge effect also occurs when a tool penetrates through the bottom surface of a workpiece, even if there is nothing underneath or if the workpiece is simply stacked on top of another piece of metal. It can be used to fabricate a negative taper at the end of a deep microhole [29].

B. Sensing Debris-Dominated Machining

The detection of debris accumulation is essential to high-quality machining in batch-mode μ EDM. One past effort used a pulse discrimination algorithm to determine the percentage of complex (spurious) discharges over the course of machining [16]. The resulting information has the same pattern as the amplitude of the spectrogram in Fig. 4. While direct waveform measurement has been used to detect the various discharge states, it is also subject to changing parasitics from different patterns, materials, etc. For very low discharge energies, wireless sensing could provide an advantage.

Wireless measurement directly measures the discharge. Changes in the wireless spectra may provide an early warning before debris-dominated machining occurs. Dynamically adjusting machining parameters and flushing based on this feedback could then potentially improve machining efficiency and prevent workpiece and tool damage.

The formulation of models for the discharge process and for the wireless spectrum of fast-moving current pulses, such as those present in EDM, is a subject of constant experimentation and research [30]–[37]. Kadish and Maier have modeled discharges as current discontinuities within a cylindrical discharge channel [19]. Fujiwara *et al.* simulated a 2-mm discharge between metal spheres with a finite-difference time-domain method to obtain predicted electric and magnetic-field traces [37]. There has been little work in modeling discharges at gaps in the micrometer range. This may be a direction for extensive future effort because the plasma physics change significantly when the discharge gap is scaled down [38], [39]. Debris in the discharge gap and variations in surface geometry will also have much larger roles at these scales.

V. CONCLUSION

Inherent wireless-signal information from the discharges in μ EDM can be very helpful in monitoring machining progress and discharge quality. The information gathered is directly related to the discharge and complements voltage and current information from terminal-probe measurements. The metal-metal interface transition between stainless steel and electroplated copper has shown a 10-dBm shift in intensity for the 300–350-MHz band and a 5-dBm average change across the full 1-GHz bandwidth. This technique can be applied to separate stacked metals as well. As debris accumulate in batch-mode μ EDM, the signal amplitude decreases across the spectrum. The experiments have typically shown a 4-dBm drop in the 800–850-MHz band with a 2.2-dBm average drop across the full 1-GHz bandwidth. Wireless monitoring could potentially be used with μ EDM control hardware to monitor multiple machines at once. This paper paves the way for comprehensive studies utilizing more complicated patterns and practical test cases.

ACKNOWLEDGMENT

The authors would like to thank Dr. K. Takahata for evaluating the impact of debris accumulation on batch-mode μ EDM.

REFERENCES

- [1] T. Masaki, K. Kawata, and T. Masuzawa, "Micro electro-discharge machining and its applications," in *Proc. IEEE Int. Conf. Micro Electro Mech. Syst.*, 1990, pp. 21–26.
- [2] K. Takahata and Y. B. Gianchandani, "Batch mode micro-electro-discharge machining," *J. Microelectromech. Syst.*, vol. 11, no. 2, pp. 102–110, Apr. 2002.
- [3] K. Udeshi and Y. B. Gianchandani, "A DC-powered high-voltage generator using a bulk Pt.Rh oscillating micro-relay," in *Proc. IEEE Int. Conf. Solid State Sens., Actuators, Microsyst., TRANSDUCERS*, 2007, pp. 1151–1154.
- [4] T. Fofonoff, S. M. Martel, N. G. Hatsopoulos, J. P. Donoghue, and I. W. Hunter, "Microelectrode array fabrication by electrical discharge machining," *IEEE Trans. Biomed. Eng.*, vol. 51, no. 6, pp. 890–895, Jun. 2004.
- [5] K. Takahata and Y. B. Gianchandani, "Micromachined antenna stents and cuffs for monitoring intraluminal pressure and flow," *J. Microelectromech. Syst.*, vol. 15, no. 5, pp. 1289–1298, Oct. 2006.
- [6] K. Takahata, "Batch manufacturing technology based on micro-electro-discharge machining and application to cardiovascular stents," Ph.D. dissertation, Univ. Michigan, Ann Arbor, MI, 2005.
- [7] B. Kloeck, S. D. Collins, N. F. de Rooij, and R. L. Smith, "Study of electrochemical etch-stop for high-precision thickness control of silicon membranes," *IEEE Trans. Electron Devices*, vol. 36, pt. 2, no. 4, pp. 663–669, Apr. 1989.
- [8] H. El-Hofy, *Advanced Machining Processes: Nontraditional and Hybrid Machining Processes*. New York: McGraw-Hill, 2005, pp. 115–139.
- [9] J. A. McGeough, *Advanced Methods of Machining*. New York: Chapman & Hall, 1988, pp. 128–152.
- [10] J. Brown, *Advanced Machining Technology Handbook*. New York: McGraw-Hill, 1998, pp. 116–130.
- [11] M. T. Richardson and Y. B. Gianchandani, "Achieving precision in high density batch mode micro-electro-discharge machining," *J. Micromech. Microeng.*, vol. 18, no. 1, pp. 1–12, Jan. 2008.
- [12] R. Tobazeon, "Electrohydrodynamic behaviour of single spherical or cylindrical conducting particles in an insulating liquid subjected to a uniform DC field," *J. Phys. D, Appl. Phys.*, vol. 29, no. 10, pp. 2595–2608, Oct. 1996.
- [13] I. Cabanes, E. Portillo, M. Marcos, and J. A. Sanchez, "An industrial application for on-line detection of instability and wire breakage in wire EDM," *J. Mater. Process. Technol.*, vol. 195, no. 1–3, pp. 101–109, Jan. 2008.

- [14] H. S. Liu and Y. S. Tarn, "Monitoring of the electrical discharge machining process by abductive networks," *Int. J. Adv. Manuf. Technol.*, vol. 13, no. 4, pp. 264–270, Apr. 1997.
- [15] C.-C. Kao, A. J. Shih, and S. F. Miller, "Fuzzy logic control of microhole electrical discharge machining," *J. Manuf. Sci. Eng.*, vol. 130, no. 6, pp. 064 502:1–064 502:6, Dec. 2008.
- [16] Y. S. Liao, T. Y. Chang, and T. J. Chuang, "An on-line monitoring system for a micro electrical discharge machining (micro-EDM) process," *J. Micromech. Microeng.*, vol. 18, no. 3, pp. 1–8, Mar. 2008.
- [17] D. J. Kim, S. M. Yi, Y. S. Lee, and C. N. Chu, "Straight hole micro EDM with a cylindrical tool using a variable capacitance method accompanied by ultrasonic vibration," *J. Micromech. Microeng.*, vol. 16, no. 5, pp. 1092–1097, May 2006.
- [18] S. Ishigami and T. Iwasaki, "Evaluation of charge transition in a small gap discharge," *IEICE Trans. Commun.*, vol. 79B, no. 4, pp. 474–482, Apr. 1996.
- [19] A. Kadish and W. B. Maier, "Electromagnetic radiation from abrupt current changes in electrical discharges," *J. Appl. Phys.*, vol. 70, no. 11, pp. 6700–6711, Dec. 1, 1991.
- [20] H. Tomita, "Dependence of current and induced voltage due to spark discharge on gap length," in *Proc. Int. Symp. Electromagn. Compat.*, 1999, pp. 138–141.
- [21] Y. Ebara, T. Koizumi, H. Sone, and Y. Nemoto, "Experiments on relationship between electromagnetic noise and surface profile change by arc discharge of heterogeneous material contacts," in *Proc. IEEE Int. Symp. Electromagn. Compat.*, 1999, pp. 165–170.
- [22] Y. Ebara, H. Sone, and Y. Nemoto, "Correlation between arcing phenomena and electromagnetic noise of opening electric contacts," in *Proc. IEEE Elect. Contacts*, 2000, pp. 191–197.
- [23] S. K. Bhattacharyya and M. F. El-Menshawy, "Monitoring the E.D.M. process by radio signals," *Int. J. Prod. Res.*, vol. 16, no. 5, pp. 353–363, Sep. 1978.
- [24] S. K. Bhattacharyya and M. F. El-Menshawy, "Monitoring and controlling the E.D.M. process," *Trans. ASME, J. Eng. Ind.*, vol. 102, pp. 189–194, Aug. 1980.
- [25] M. T. Richardson, R. Gharpurey, and Y. B. Gianchandani, "Wireless sensing of discharge characteristics for quality control in batch mode micro-electro-discharge machining," in *Proc. Solid State Sens. Actuators Workshop*, Hilton Head Island, SC, 2006, pp. 404–407.
- [26] M. T. Richardson and Y. B. Gianchandani, "Real-time wireless monitoring of workpiece material and debris characteristics in micro-electro-discharge machining," in *Proc. IEEE Int. Conf. Micro Electro Mech. Syst.*, 2008, pp. 379–382.
- [27] W. Kurnia, P. C. Tan, S. H. Yeo, and M. Wong, "Analytical approximation of the erosion rate and electrode wear in micro electrical discharge machining," *J. Micromech. Microeng.*, vol. 18, no. 8, pp. 1–8, Aug. 2008.
- [28] M. T. Richardson, "High resolution lithography-compatible micro-electro-discharge machining of bulk metal foils for micro-electro-mechanical systems," Ph.D. dissertation, Univ. Michigan, Ann Arbor, MI, 2009.
- [29] C.-C. Kao, "Monitoring and control of micro-hole electrical discharge machining," Ph.D. dissertation, Univ. Michigan Press, Ann Arbor, MI, 2007.
- [30] G. V. Naidis, "Simulation of streamer-to-spark transition in short non-uniform air gaps," *J. Phys. D, Appl. Phys.*, vol. 32, no. 20, pp. 2649–2654, Oct. 1999.
- [31] P. Shankar, V. K. Jain, and T. Sundararajan, "Analysis of spark profiles during EDM process," *Mach. Sci. Technol.*, vol. 1, no. 2, pp. 195–217, Dec. 1997.
- [32] P. F. Wilson, "Fields radiated by electrostatic discharges," *IEEE Trans. Electromagn. Compat.*, vol. 33, no. 1, pp. 10–18, Feb. 1991.
- [33] W. D. Greason, Z. Kucerovsky, M. W. Flatley, and S. Bulach, "Non-invasive measurement of electrostatic discharge induced phenomena in electronic systems," *IEEE Trans. Ind. Appl.*, vol. 34, no. 3, pp. 571–579, May/Jun. 1998.
- [34] M. Takeuchi and T. Kubono, "Experiment on the radiated magnetic field caused by a breaking arc," *IEICE Trans. Commun.*, vol. E79-B, no. 4, pp. 503–508, Apr. 1996.
- [35] I.-H. Kang, O. Fujiwara, and C.-B. Lee, "Spectrum distribution of electromagnetic field radiated by electrostatic discharge on the ground screen," in *Proc. Int. Symp. Electromagn. Compat.*, 1998, vol. 2, pp. 994–998.
- [36] S. Dhanik and S. S. Joshi, "Modeling of a single resistance capacitance pulse discharge in micro-electro-discharge machining," *J. Manuf. Sci. Eng.*, vol. 127, no. 4, pp. 759–767, Nov. 2005.
- [37] O. Fujiwara, K. Okuda, K. Fukunaga, and Y. Yamanaka, "FDTD computation of electromagnetic fields caused by electrostatic discharge between charged metal spheres," *Electron. Commun. Jpn.*, vol. 86, pt. 1, no. 7, pp. 54–63, Jul. 2003.
- [38] C. G. Wilson, Y. B. Gianchandani, R. R. Arslanbekov, V. Kolobov, and A. E. Wendt, "Profiling and modeling of dc nitrogen microplasmas," *J. Appl. Phys.*, vol. 94, no. 5, pp. 2845–2851, Sep. 2003.
- [39] M. J. Kushner, "Modelling of microdischarge devices: Plasma and gas dynamics," *J. Phys. D, Appl. Phys.*, vol. 38, no. 11, pp. 1633–1643, Jun. 2005.



Mark T. Richardson (M'09) received the B.S. (*magna cum laude*), M.S., and Ph.D. degrees in electrical engineering from the University of Michigan, Ann Arbor, in 2004, 2006, and 2009 respectively, with a focus on circuits and microsystems.

He is currently working at Raytheon Space and Airborne Systems. He has interned at Sandia National Laboratories, CA, and the NSF ERC for Wireless Integrated Microsystems (WIMS). His research interests include batch mode micro-electro-discharge machining, implantable medical devices, and power circuits. He has nine publications in MEMS and μ EDM research.

Dr. Richardson received the DeVlieg fellowship in manufacturing technology in 2004.



Yogesh B. Gianchandani (S'83–M'85–SM'04) received the B.S., M.S., and Ph.D. degrees in electrical engineering, with a focus on microelectronics and MEMS. He is presently a Professor at the University of Michigan, Ann Arbor, with a primary appointment in the Electrical Engineering and Computer Science Department and a courtesy appointment in the Mechanical Engineering Department. He is temporarily serving at the National Science Foundation, as the program director within the Electrical, Communication, and Cyber Systems Division (ECCS).

Dr. Gianchandani's research interests include all aspects of design, fabrication, and packaging of micromachined sensors and actuators and their interface circuits (<http://www.eecs.umich.edu/~yogesh/>). He has published approximately 200 papers in journals and conferences, and has about 30 U.S. patents issued or pending. He was a Chief Co-Editor of *Comprehensive Microsystems: Fundamentals, Technology, and Applications*, published in 2008. He serves several journals as an editor or a member of the editorial board, and served as a General Co-Chair for the IEEE/ASME International Conference on Micro Electro Mechanical Systems (MEMS) in 2002.